HHS Public Access

Author manuscript

J Allergy Clin Immunol. Author manuscript; available in PMC 2024 January 12.

Published in final edited form as:

J Allergy Clin Immunol. 2023 June ; 151(6): 1536–1549. doi:10.1016/j.jaci.2023.01.030.

Type 2 inflammation drives an airway basal stem cell program through insulin receptor substrate signaling

Xin Wang, PhD[a,b], **Nils R. Hallen, BS**[a,b], **Minkyu Lee, PhD**[a,b], **Sachin Samuchiwal, PhD**[a,b], **Qihua Ye, MS**[a,b], **Kathleen M. Buchheit, MD**[a,b], **Alice Z. Maxfield, MD**[c], **Rachel E. Roditi, MD**[c], **Regan W. Bergmark, MD**[c], **Neil Bhattacharyya, MD**[d], **Tessa Ryan, BA**[a,b], **Deb Gakpo, BA**[a,b], **Soumya Raychaudhuri, MD, PhD**[e,f,g,h,i], **Dan Dwyer, PhD**[a,b], **Tanya M. Laidlaw, MD**[a,b], **Joshua A. Boyce, MD**[a,b], **Maria Gutierrez-Arcelus, PhD**[h,j], **Nora A. Barrett, MD**[a,b]

[a]Jeff and Penny Vinik Center for Translational Immunology Research, Division of Allergy and Clinical Immunology, Brigham and Women's Hospital, Boston

[b]Department of Medicine, Harvard Medical School, Boston

[c]Department of Otolaryngology, Head and Neck Surgery, Brigham and Women's Hospital, Boston

[d]Department of Otolaryngology, Head and Neck Surgery, Massachusetts Eye and Ear Infirmary, Boston

[e]Center for Data Sciences, Brigham and Women's Hospital, Boston

[f]Division of Genetics, Brigham and Women's Hospital and Harvard Medical School, Boston

[g]Division of Rheumatology, Inflammation, and Immunity, Department of Medicine, Brigham and Women's Hospital and Harvard Medical School, Boston

[h]Program in Medical and Population Genetics, Broad Institute of MIT and Harvard, Cambridge

[i]Versus Arthritis Centre for Genetics and Genomics, Centre for Musculoskeletal Research, Manchester Academic Health Science Centre, University of Manchester, Manchester

[j]Division of Immunology, Boston Children's Hospital, Boston

Abstract

Background: Chronic rhinosinusitis with nasal polyposis (CRSwNP) is a type 2 (T2) inflammatory disease associated with an increased number of airway basal cells (BCs). Recent studies have identified transcriptionally distinct BCs, but the molecular pathways that support or inhibit human BC proliferation and differentiation are largely unknown.

Objective: We sought to determine the role of T2 cytokines in regulating airway BCs.

Corresponding author: Nora A. Barrett, MD, Hale Building for Transformative Medicine, Room 05002R, 60 Fenwood Rd, Boston, MA 02115. nbarrett@bwh.harvard.edu.

Disclosure of potential conflict of interest: J. A. Boyce has served on scientific advisory boards for Siolta Therapeutics, Third Harmonic Bio, and Sanofi/Aventis. N. A. Barrett has served on scientific advisory boards for Regeneron. K. M. Buchheit has served on scientific advisory boards for AstraZeneca, Regeneron, Sanofi, and GlaxoSmithKline. T. M. Laidlaw has served on scientific advisory boards for Regeneron, Sanofi, and GlaxoSmithKline. The rest of the authors declare that they have no relevant conflicts of interest.

Methods: Single-cell and bulk RNA sequencing of sinus and lung airway epithelial cells was analyzed. Human sinus BCs were stimulated with IL-4 and IL-13 in the presence and absence of inhibitors of IL-4R signaling. Confocal analysis of human sinus tissue and murine airway was performed. Murine BC subsets were sorted for RNA sequencing and functional assays. Fate labeling was performed in a murine model of tracheal injury and regeneration.

Results: Two subsets of BCs were found in human and murine respiratory mucosa distinguished by the expression of basal cell adhesion molecule (BCAM). BCAM expression identifies airway stem cells among $P63^{+}KRT5^{+}NGFR^{+}$ BCs. In the sinonasal mucosa, $BCAM^{hi}$ BCs expressing *TSLP, IL33, CCL26*, and the canonical BC transcription factor *TP63* are increased in patients with CRSwNP. In cultured BCs, IL-4/IL-13 increases the expression of *BCAM* and *TP63* through an insulin receptor substrate–dependent signaling pathway that is increased in CRSwNP.

Conclusions: These findings establish BCAM as a marker of airway stem cells among the BC pool and demonstrate that airway epithelial remodeling in T2 inflammation extends beyond goblet cell metaplasia to the support of a BC stem state poised to perpetuate inflammation. (J Allergy Clin Immunol 2023;151:1536-49.)

GRAPHICAL ABSTRACT

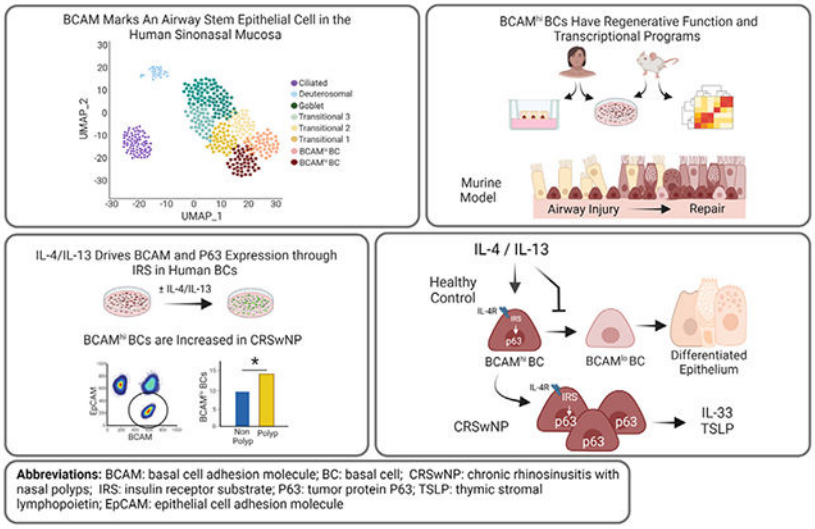

Keywords

Basal cell; airway stem cell; basal cell adhesion molecule; airway inflammation; type 2 inflammation; IL-4; IL-13; chronic rhinosinusitis with nasal polyposis; asthma; single-cell RNA sequencing

Tissue-resident stem cells exhibit remarkable plasticity, responding to local damage by regenerating diverse differentiated cell types. This plasticity ensures their ability to restore homeostasis after injury but also endows them with the capacity to remodel the tissue microenvironment and adapt to tissue stress. A canonical example of tissue remodeling is intestinal goblet cell metaplasia, which plays an essential role in host defense against helminths. Here, local immunocytes generate IL-13, which drives the differentiation of

epithelial cells (EpCs) into goblet cells that secrete mucus and thereby facilitate helminth expulsion.[1–3] Although appropriate tissue adaptation requires that stem cells integrate local environmental cues from diverse sources including niche mesenchymal cells, tissue immunocytes, and even their own progeny, in most circumstances the signals that mediate remodeling and the features of remodeling that are beneficial or detrimental to the host are poorly understood.

In the respiratory tract, studies using single-cell RNA sequencing (scRNA-seq) and immunofluorescence have identified variations in the abundance of EpC subsets in distinct disease states. This includes an expansion of ciliated cells in cystic fibrosis,[4] an increase in IL-25–secreting tuft cells in allergic fungal rhinosinusitis and chronic rhinosinusitis with nasal polyposis (CRSwNP),[5–7] and an increase in neuroendocrine cells in diffuse idiopathic pulmonary neuroendocrine cell hyperplasia,[8–10] asthma,[11] and neuroendocrine cell hyperplasia of infancy.[12] These specialized EpCs derive from basal cell (BC) progenitors, suggesting that alterations in BC programs likely account for these variations. Indeed, scRNA-seq has detected transcriptionally distinct BC subsets in the respiratory tract,[13–15] but functional annotation of these cell types is lacking.

In Western countries, CRSwNP is a type 2 (T2) inflammatory disease of the sinonasal airway that is often associated with asthma. Patients with this disorder have eosinophilia in the airways and peripheral blood and respond to treatment with mAb blockade of IL-4Rα, a component of both the T1 and T2 IL-4 receptors that bind IL-4 and IL-13.[16] We previously reported that BCs from patients with CRSwNP accumulated in the sinonasal mucosa and failed to differentiate normally, but the mechanism by which this occurs is unknown.

Here, we report 2 subsets of $KRT5^+$ BCs in the sinonasal mucosa distinguished by expression of basal cell adhesion molecule (BCAM). Using sequencing, *ex vivo* culture, and *in vivo* experimentation, we demonstrate that $BCAM^{hi}$ BCs are the progenitors of $BCAM^{lo}$ BCs, that they increase in CRSwNP, and that the T2 cytokines IL-4 and IL-13 reinforce the expression of BCAM and prevent BC differentiation through an insulin receptor substrate (IRS)–dependent signaling pathway that is overexpressed in CRSwNP. These findings demonstrate that IL-4/IL-13 can play a profound role in remodeling the airway epithelial BC compartment to drive the accumulation of a stem cell with potent proinflammatory capacity.

METHODS

Study design

This study was designed to characterize BC subsets in the human and murine airway and to understand the alterations in BC programs in T2 inflammatory diseases such as CRSwNP. This objective was addressed by (1) reanalysis of scRNA-seq[13] of nonproliferating surface airway EpCs in surgical excisions of human sinonasal mucosa from patients with CRSwNP (n = 6) and those with chronic rhinosinusitis sans nasal polyposis (CRSsNP) (n = 6) to identify potential markers of BC subsets; (2) flow-cytometric analysis and *ex vivo* studies of primary human sinonasal BCs from subjects with chronic rhinosinusitis or healthy control subjects to demonstrate distinct BC functions; (3) development of a murine flow-cytometry

panel, bulk RNA-seq data sets, BC lineage-tracing system, and a model of airway damage and regeneration to characterize BC subsets in C57BL/6 mice; and (4) assessment of human BCAM^{hi} BCs *ex vivo* with and without T2 cytokines. Details of the subjects; analytic methods for scRNA-seq and bulk RNA-seq; protocols for cell isolation, staining, and culture; methods for confocal analysis; and murine *Alternaria alternata* (ALT) challenges are provided in this article's Online Repository at www.jacionline.org.

Study approval

The Mass General Brigham Institutional Review Board approved the study, and all subjects provided written informed consent before participation. The use of mice for this study was in accordance with the review and approval by the Animal Care and Use Committee of Brigham and Women's Hospital.

Data and code availability

Low-input RNA-seq data have been deposited in the Gene Expression Omnibus (GSE197274). CRSwNP single-cell data set has been deposited in ImmPort SDY1877. The public data set from healthy lung was downloaded from https://www.covid19cellatlas.org/index.healthy.html#vieira19-bronchi.[14] The code for main analyses is available at https://github.com/nils-hallen/Single-Cell-Analyses.

Statistical analysis

Computational methods for RNA sequencing are detailed in this article's Online Repository at www.jacionline.org. Other analyses were performed with the GraphPad Prism software (version 9.3.1, GraphPad, La Jolla, Calif) and R (version 4.03). All *in vitro* and *in vivo* results are either representative of or pooled across 3 to 5 independent experiments. Data indicate mean ± SEM in all bar graphs. A P value of less than .05 was considered significant.

RESULTS

BCAM marks a multipotent progenitor cell among KRT5$^+$NGFR$^+$ITGA6$^+$ BCs in the human respiratory mucosa

We previously reported the impaired differentiation of airway EpCs in patients with CRSwNP.[13] To better delineate EpC differentiation, we reanalyzed our scRNA-seq data set from sinus surgeries.[13] Using Harmony,[17] we integrated data across donors and patient subtypes (CRSsNP and CRSwNP) in principal-component space, reclustered nonproliferating surface airway secretory and ciliated EpCs (see Fig E1, A–D, and Tables E1–E3 in this article's Online Repository at www.jacionline.org), and assessed established EpC markers (Table I) to define common EpC states across diseases (Fig E1, E). Here, we identified 2 BC subsets present in the sinonasal tissue of patients with CRSwNP and those with CRSsNP (Fig 1, A–C). One subset (cluster 0) expressed high levels of the BC markers *KRT5, KRT15*, and *TP63*[18–20]; the stem marker *CD44*[21]; and the cell surface receptor *BCAM* (false-discovery rate < 0.05; Fig 1, B and C; see also Table E4 in this article's Online Repository at www.jacionline.org). The second BC subset (cluster 1) expressed higher levels of the oncogene *MALAT1*[22] and many ribosomal genes, suggesting ribosomal biogenesis.

Differentiating transitional cells (clusters 2-4) were marked by increasing expression of the Notch pathway gene *HES1*,[23] the luminal BC marker *KRT8*,[24] and the club cell markers *SCGB1A1* and *TFF3*,[25,26] whereas mature secretory cells (cluster 5) were marked by *MUC5AC*,[14] deuterosomal cells (cluster 6) were marked by *CDC20B, PLK4*, and *FOXJ1*,[27] and ciliated cells (cluster 7) were marked by *PIFO, CAPS*, and *FOXJ1*.[15] Cluster 5 was composed of both goblet and club secretory cells expressing *MUC5AC* or *MUC5B* and *SCGB1A1*, respectively (Fig E1, F).

Trajectory analysis of these clusters suggested 2 distinct trajectories with a serial progression from *TP63*^{hi} BC progenitors (cluster 0) to *MALAT1*$^{+}$ BCs (cluster 1), *KRT8*$^{+}$ *HES1*^{hi} transitional cells (clusters 2-4), and then to either fully differentiated *MUC5AC*$^{+}$ goblet cells (cluster 5) or to *PIFO*$^{+}$ ciliated EpCs (cluster 7) (Fig 1, D and E). Accordingly, cells in the secretory trajectory from clusters 0 to 5 (Fig E1, G) demonstrated progressively increasing pseudotime scores (Fig 1, F). Using generalized linear modeling across pseudotime for EpCs in the secretory trajectory, we demonstrated 2278 genes that were either highly positively or negatively associated with the pseudotime score ($P < 4.23 \times 10^{-6}$, Bonferroni threshold; Fig 1, G; see also Tables E5 and E6 in this article's Online Repository at www.jacionline.org). We detected increasing expression of canonical secretory genes across pseudotime and loss of BC markers, as expected (Fig 1, G). In addition, we saw that expression of the cluster 0 BC marker *BCAM* (Fig 1, C) was inversely associated with pseudotime, suggesting that its expression may distinguish states of BC differentiation.

Direct comparison of cluster 0 BCAM^{hi} BCs and cluster 1 BCAM^{lo} BCs demonstrated 142 genes that were differentially expressed between these clusters ($P < 1.5 \times 10^{-5}$, Bonferroni threshold; Fig 1, H; see also Table E7 in this article's Online Repository at www.jacionline.org). BCAM^{hi} BCs expressed higher levels of many genes associated with epithelial progenitor cells. These included the Yap target gene *CYR61/CCN1*,[28] WNT target genes *MMP10*[29] and *MYC*,[30] the NOTCH ligand *DLL1*[31] and the NOTCH inhibitor *DLK2*,[32] the proliferation-associated gene *ZFP36L2*,[33] and transcription factors required for stem cell maintenance, such as *TCF12*[34] and *TP63*.[19,20,35] BCAM^{hi} BCs also expressed higher levels of the T2 cytokine and transcriptional repressor *IL33*[36,37] and showed a trend to increased *TSLP* that was not significant after Bonferroni adjustment. In addition, BCAM^{hi} BCs expressed higher levels of genes encoding growth factors and extracellular matrix components such as *POSTN* (periostin), *FN1* (fibronectin), *CTGF* (connective tissue growth factor), *LAMB1* (laminin subunit B1), and *LAMB3* (laminin subunit B3). In contrast, BCAM^{lo} BCs expressed higher levels of genes associated with differentiation, including *SERPINB3*,[38] *HES1*[23] *KRT8*,[31] and the transcription factor *ELF3*,[39,40] suggesting that increased *BCAM* expression identifies early airway progenitors among the BC pool.

Confocal images of the epithelium in CRSwNP confirmed variable expression of BCAM, with some KRT5^{+} BCs expressing BCAM solely on the basal surface (designated BCAM^{lo}) and other KRT5^{+} BCs expressing BCAM circumferentially (designated BCAM^{hi}) (Fig 1, I, top row). BCAM^{hi} BCs expressed p63 (Fig 1, I, second row), IL-33 (Fig 1, I, third row), and Ki67 (Fig 1, l, fourth row), but none of these proteins was exclusively expressed in BCAM^{hi} BCs. Flow cytometry also demonstrated variable BCAM expression among EpCAM^{lo}NGFR^{hi} BCs (Fig E1, H). Remarkably, both BCAM^{hi} and BCAM^{lo} BCs had

similar staining for integrin alpha 6,[18,41] and little distinction in the expression levels of the BC markers podoplanin[31] and nerve growth factor receptor (NGFR)[18] (Fig E1, I). Sorted BCAM^{hi} BCs were passaged and differentiated in air-liquid interface (ALI) cultures that supported the growth of all common EpC subsets (Fig 1, J and K). In contrast, EpCAM^{lo}NGFR^{hi}BCAM^{lo} BCs survived only limited passages ex vivo and could not support differentiation in ALI cultures. Taken together, these results suggested that BCAM expression distinguishes sinonasal stem cells among BCs.

Notably, examination of a published scRNA-seq data set from bronchial mucosa[14] revealed that *BCAM* also marks a subset of bronchial BCs from healthy donors with coexpression of *TP63* and *IL33* (Fig E1, J). After assessment of differential gene expression between BCAM^{hi} and BCAM^{lo} bronchial BCs, we analyzed differentially expressed genes that were detected in both the bronchial and the polyp BC subsets. This demonstrated a strong correlation in gene programs across data sets (Fig 1, L; see also Table E8 in this article's Online Repository at www.jacionline.org), indicating that a similar BCAM^{hi} BC population exists in the lower airway.

BCAM marks an airway stem cell among KRT5^{+}NGFR^{+}ITGA6^{+}P63^{+} BCs in the murine trachea

The limited progenitor capacity of BCAM^{lo} BCs in *ex vivo* culture was striking, because even differentiated club cells are reported to retain some progenitor capacity in the appropriate context.[42,43] Thus, we next sought to assess these populations *in vivo* and turned to the murine airway. In the sinonasal mucosa (see Fig E2, A, in this article's Online Repository at www.jacionline.org) and in the trachea (Fig 2, A), confocal microscopy demonstrated 2 patterns of BCAM staining on basal EpCs, with circumferential expression of BCAM on some BCs and focal basolateral expression of BCAM on other BCs. P63 was primarily expressed in BCAM^{hi} BCs, consistent with a BC progenitor. Because BC biology and markers are more clearly established in the trachea, we next adapted a flow-cytometric panel to assess BCAM expression in naive tracheal BCs. Within the conventional BC gate (lin^{-}EpCAM^{lo}GSIB4^{hi}),[44,45] we again identified 2 EpC subsets distinguished by BCAM expression (Fig 2, B; see also Fig E2, B). Both populations expressed lower levels of EpCAM and higher levels of BC markers than did differentiated EpCs (Fig 2, C and D). Neither BC subset expressed markers of specialized differentiated EpCs (Fig E2, C–E). Notably, KI67^{+} staining was dominantly detected in BCAM^{hi} BCs, which was confirmed by confocal microscopy (Fig 2, E). To directly assess their proliferative capacity, we first sorted tracheal BCAM^{hi} and BCAM^{lo} BCs and expanded them in submerged culture (Fig 2, F and G). BCAM^{hi} BCs formed larger Ki67^{+} and P63^{+} colonies and were more efficient at closing a wound than were BCAM^{lo} BCs (Fig 2, G and H). Thus, both classical markers of replication and functional assays for proliferation and wound healing demonstrated that BCAM distinguishes a murine airway stem cell among KRT5^{+} BCs.

EpCs differentiate from BCAM^{hi} to BCAM^{lo} BCs in a model of airway injury and inflammation

Having established the *ex vivo* behavior of murine BCAM^{hi} and BCAM^{lo} BCs, we next assessed their behavior in a murine model of airway inflammation and injury using

the repetitive inhalation of the mold aeroallergen ALT over 1 or 2 weeks (Fig 3, A). Hematoxylin and eosin staining demonstrated epithelial injury by day 7 and regeneration by day 14 (Fig 3, B). Regeneration was accompanied by a shift in the dominant BC population from BCAM^{hi} at day 0 to BCAM^{int} (intermediate) at day 7 and BCAM^{lo} at day 14 (Fig 3, C). After these repetitive challenges, some BCAM^{lo} BCs expressed the secretory markers SSEA1 and MUC5AC (Fig 3, D; see also Fig E3, A, in this article's Online Repository at www.jacionline.org), suggesting early differentiation. In contrast, BCAM^{hi} BCs did not express markers of differentiation and were the dominant cell type expressing Ki67 at all time points (Fig 3, E; see also Fig E3, B and C). Taken together, these results suggested that BCAM marks a renewable stem progenitor responsive to airway injury, and that BCAM^{hi} BCs may give rise to BCAM^{lo} BCs and then to differentiated EpCs.

To confirm that BCAM^{hi} BCs are the progenitors of BCAM^{lo} BCs, we performed fate mapping using tamoxifen-treated, ALT-challenged KRT5^{CreERT2}R26^{tdTomato} mice. Mice were treated with 5 doses of tamoxifen to label KRT5^{+} BCs, rested for 1 week, and then treated with intranasal ALT over 1 or 2 weeks (Fig 3, A). As expected, the percentage of EpCs labeled with tdTomato increased over the ALT challenges (Fig 3, F and G), and although most tdTomato^{+} cells were detected in the BCAM^{hi} BC gate at day 7, over the ALT challenges an increasing number fell in the BCAM^{lo} BC gate and then the differentiated EpC gate (Fig 3, H; see also Fig E3, D–F). These data are consistent with an EpC differentiation trajectory that begins with BCAM^{hi} BCs and progresses to BCAM^{lo} BCs and then to differentiated EpCs.

Transcriptional profile of murine BCAM^{hi} and BCAM^{lo} BCs

Because our low-resolution scRNA-seq provided only a limited assessment of these BC subsets that displayed such distinct *ex vivo* and *in vivo* behaviors, we next isolated them from naive murine trachea and assessed their transcriptional differences with bulk RNA-seq (see Fig E4, A, in this article's Online Repository at www.jacionline.org). Principal-component analysis demonstrated that PC1 separated samples by stage of differentiation (Fig 4, A; see also Table E9 in this article's Online Repository at www.jacionline.org). Direct comparison of BCAM^{hi} and BCAM^{lo} BCs demonstrated that BCAM^{hi} BCs expressed higher levels of many of the same markers detected at elevated levels in human BCAM^{hi} BCs including *Krt5, Trp63, Ccn1* (*CYR61*), *Lamb3, Jag2, Dlk2*, and *Bcam*, and higher levels of additional BC markers *Ngfr, Pdpn, Krt14*, and *Krt17* (FDR < 0.05; Fig 4, B and C; see also Fig E4, B, and Tables E10 and E11 in this article's Online Repository at www.jacionline.org). *Il33* was poorly detected in each group. BCAM^{hi} and BCAM^{lo} BCs expressed significantly different levels of genes critical for EpC differentiation and maintenance of stemness, including genes in the Wnt (Fig 4, D), Hippo-Yap (Fig 4, E), Notch (Fig 4, F), Rho (Fig 4, G), and Ras (Fig 4, H) pathways. Although only a few genes in each of these pathways were recovered in the human scRNA-seq data set, all but one of them (*CCND1*) were significantly increased in BCAM^{hi} BCs, as compared with BCAM^{lo} BCs (Fig E4, C). Transcription factors that were significantly different in the murine data included the regulator of embryonic morphogenesis *Hoxd8*[46]; the driver of respiratory and epidermal BC proliferation *Vdr*[47,48]; the tumor suppressors *Klf10, Klf11*, and *Trp53*[49–51]; and 17 transcripts encoding zinc-finger proteins, all of which were

increased in BCAM^{hi} BCs (Fig E4, D; see also Table E12 in this article's Online Repository at www.jacionline.org). Among the top transcription factors differentially regulated was *Trp63* (Fig E4, D), the murine homologue of *TP63* that was detected in human sinonasal BCAM^{hi} BCs (Fig 1, C, and H). Assessment of a previously reported list of 175 genes with *p63* binding sites[52] showed that 34 were differentially expressed across BCAM^{hi} and BCAM^{lo} BC subsets (Fig 4, I). Moreover, 10 were among the top 250 genes upregulated in BCAM^{hi} BCs, suggesting a potential link between *BCAM* and *Trp63*. Assessment of our previously published bulk RNA-seq data set from human sinonasal BCs from CRSwNP demonstrated strong correlation between *BCAM* expression and *TP63* ($r^2 = 0.85$; $P = .001$; Fig 4, J; see also Table E13 in this article's Online Repository at www.jacionline.org), suggesting a potential link between *BCAM* and *TP63* expression in human BCs.

T2-/IRS-dependent regulation of BCAM

TP63 was previously reported to be induced by the T2 cytokine IL-13 in human keratinocytes,[53] and thus we hypothesized that *BCAM* may be similarly regulated in the sinonasal mucosa. First, we assessed *BCAM* and *TP63* expression in bulk RNA-seq of sinonasal BCs from CRSwNP, a T2-high disease, and from nonpolyp controls (CRSsNP). Polyp BCs expressed higher levels of *BCAM* and *TP63* and higher levels of canonical T2-inducible epithelial genes such as *ALOX15, POSTN, IL33*, and *TSLP* (Fig 5, A; see also Table E14 in this article's Online Repository at www.jacionline.org). There was a trend to increased expression of *CCL26* that was not significant. In addition, flow cytometry demonstrated that the percentage of BCAM^{hi} BCs among lin $^{-}$EpCAM^{lo}NGFR^{+} cells was higher in CRSwNP than in CRSsNP (Fig 5, B). Interestingly, assessment of p63-dependent genes also showed an increase in BCs from CRSwNP, as compared with CRSsNP (Fig 5, C), suggesting an increase in the p63-dependent stem program in this T2 disease.

To understand whether BCAM and p63 were directly regulated by T2 cytokines, we cultured sinonasal BCs from healthy controls and from patients with CRSsNP or CRSwNP and treated them with either IL-4 and IL-13 or with TGF-β, which is known to induce EpC differentiation.[54] In passaged unstimulated BC cultures, BCAM was expressed at high levels in all BCs with no BCAM^{lo} BC subset detected (Fig E5, A, in this article's Online Repository at www.jacionline.org). Addition of TGF-β downregulated the expression of BC markers NGFR and ITGA6, as expected, and also downregulated the expression of *BCAM* (Fig E5, B). In contrast, IL-4/IL-13 upregulated BCAM expression but reduced NGFR and had little effect on ITGA6 (Fig 6, A). IL-4/IL-13 treatment also upregulated *TP63* and reduced expression of *HEY1*, indicating downregulation of Notch activity, which is essential for BC differentiation into secretory EpCs.[23,31] Accordingly, we saw reduced *SCGB1A1* that marks secretory club cells (Fig 6, B). Additional markers of terminal EpC differentiation were not altered in this short-term experiment in submerged culture, including *MUC5AC, FOXJ1, IL25*, and *POU2F3* (Fig E5, C. Although the number of primary human BCAM^{lo} BCs obtained from sinus tissue was too low to ask whether IL-4/IL-13 could "reverse" differentiation and drive BCAM^{lo} BCs to BCAM^{hi} BCs, we did note that murine IL-4/IL-13–stimulated BCAM^{lo} BCs did not assume the robust wound-healing capacity of BCAM^{hi} BCs (Fig 2, H), and that *in vivo* ALT challenge was associated with increased expression of differentiation markers in BCAM^{lo} BCs (Fig 3, D). Taken together,

these findings indicate that IL-4/IL-13 reinforces a stem program in BCAM^{hi} BCs and *prevents* early steps in BC differentiation. Notably, IL-5 treatment has no such effect (Fig E5, D), possibly because of low levels of CSF2RB expression in BCs (Fig E5, E) or because of distinctions in their downstream signaling pathways.

IL-13 induces goblet cell metaplasia through a well-characterized signal transducer and activator of transcription 6 (STAT6)–dependent pathway, but STAT6-independent pathways have previously been implicated in airway epithelial wound healing.[55] Thus, we next assessed whether STAT6 or other IL-4Rα signaling pathways restrain BC differentiation. Pharmacological inhibition demonstrated that IL-4/IL-13–elicited BCAM expression was independent of STAT6 and mTOR (mammalian target of rapamycin) signaling but dependent on IRS signaling (Fig 6, C). IRS inhibition also reduced P63 expression (Fig 6, D) and the expression of BCAM and TP63 transcripts (Fig 6, E) while increasing the expression of *SCGB1A1*. Assessment of transcripts for components of the IL-4R signaling pathway in bulk BC RNA-seq demonstrated that *IL4RA* and *IRS1* were upregulated in polyp BCs, as compared with controls (Fig 6, F; see also Table E14), whereas *IRS2* showed a trend to increase that was not significant. Taken together, these data demonstrate that IL-4Rα and IRS signaling plays an unexpected role in maintaining the BCAM^{hi} BC stem state, which accumulates in CRSwNP. Finally, we did interrogate our scRNA-seq data set to assess whether BCAM^{hi} BCs from CRSwNP expressed higher levels of T2-inducible epithelial genes than did BCAM^{hi} BCs from CRSsNP. We found that although *TSLP* and *IL33* were expressed at similar levels, *POSTN, CCL26*, and *ALOX15* were expressed more highly in BCAM^{hi} BCs from CRSwNP than from CRSsNP.

DISCUSSION

Identification of airway stem cells among plastic EpC types is an important prelude to defining the molecular pathways that maintain stemness, promote normal tissue regeneration, and drive pathological tissue remodeling. Previous studies have identified human and murine airway BCs as lin^{-}EpCAM^{lo}KRT5^{+}NGFR^{hi} EpCs expressing ITGA6, PDPN, or GSIB4[13,18,56–58] and detected significant heterogeneity within the BC compartment.[4,14,24,57,59–63] However, cell surface markers to distinguish BC subsets and define BC biology have been lacking. Here, we find that BCAM expression identifies molecularly and functionally distinct subsets of BCs in human and murine airways, with BCAM^{hi} BCs expressing high levels of P63 and exhibiting increased stem functions. Remarkably, BCAM^{hi} BCs are increased in the sinonasal mucosa of patients with the T2 inflammatory disease CRSwNP, and their P63 expression is upregulated through a T2 cytokine and IRS–dependent signaling pathway. These findings identify a robust marker of airway stem cells in mouse and human and define a T2 molecular pathway that promotes their persistence.

The top marker genes identified in BCAM^{hi} BCs include *BCAM*; the keratins *KRT5, KRT15*, and *KRT17*; the canonical BC transcription factor *TP63*[19,35] and its *S100A2* target[64–66]; the stem cell regulator *MMP10*[67,68]; and diverse drivers of EpC proliferation including *LAMB3*,[69] *MYC*,[70] and the Yes-associated protein target *CYR61*.[71] Each of these transcripts marks multipotent progenitor BCs from the lower airway.[4,14,15,63,72] Moreover,

analysis of differentially expressed genes between BCAM^{hi} and BCAM^{lo} BCs from the sinus and the lung[14] demonstrates that the distinct BCAM^{hi} and BCAM^{lo} gene programs seen in the sinonasal mucosa are largely retained in the bronchial tree. Additional support for this BCAM^{hi} versus BCAM^{lo} distinction in the tracheobronchial tree is found in our murine studies. Murine tracheal BCAM^{hi} BCs, but not BCAM^{lo} BCs, express high levels of Ki67 *in vivo*, demonstrate robust colony formation and wound healing in *ex vivo* assays, and are rapidly labeled in lineagetracing studies. In addition, we found that murine tracheal BCAM^{hi} BCs are enriched in *Wnt*, *Notch*, *Rho*, and *Trp63* pathway genes expected in airway stem cells. Taken together, these findings indicate that the BCAM^{hi}/BCAM^{lo} distinction detected in the sinonasal mucosa is likely to be useful in characterizing bronchial BCs.

BCAM is a member of the immunoglobulin superfamily, broadly expressed in erythroid, epithelial, endothelial, and smooth muscle cells. BCAM binds the alpha chain of the extracellular matrix protein laminin 5[73,74] to regulate cell adhesion and migration.[75] Activation of BCAM promotes extracellular signal-regulated kinase/mitogen-activated protein kinase signaling, with an increase in RhoA and a decrease in Rac1 activity, which favors cell adhesion and colony formation in fibroblasts[76] and prevents biliary differentiation during liver regeneration.[77] Although RhoA signaling plays a central role in airway EpC differentiation,[78,79] whether BCAM is a critical regulator of BC RhoA functions will require further study. In addition, BCAM binding to laminin α5 competitively inhibits integrin binding and alters integrin-mediated functions.[80] This indicates an additional potential pathway by which BCAM expression can alter the regenerative functions of laminin α5[81,82] that are central to epithelial homeostasis and differentiation.[83,84]

Notably, we found that *BCAM* and *TP63* were both highly expressed early in pseudotime, highly correlated across BCs from subjects with CRSwNP, and similarly induced by IL-4/IL-13. Moreover, we found that human BCs from CRSwNP express higher levels of p63-dependent genes. Chromatin immunoprecipitation sequencing data demonstrate that p63 binds to a region in the BCAM promoter,[85] and a recent study identified that overexpression of *Np63* in 293T cells increases luciferase activity in a reporter containing the BCAM promoter region.[86] Thus, the reproducibility with which BCAM expression identifies airway stem cells across species and conditions may reflect its regulation by p63. Further studies are needed to understand this relationship and to understand whether targeted inhibition of IL-4Rα reduces the expression of p63 and BCAM *in vivo*.

Previous studies have identified basal luminal progenitors[24,31,57] and KRT4/13^{+} hillock BCs[59,61,72] as descendants of KRT5^{+}P63^{+} BCs that additionally express KRT8. In naive murine trachea and in human sinonasal scRNA-seq, KRT8 protein or transcript was consistently expressed in transitional EpCs, but it was not detected in either BCAM^{hi} or BCAM^{lo} BCs. Furthermore, confocal analysis demonstrated that both BCAM^{hi} and BCAM^{lo} BCs were detected on the basement membrane, distinct from KRT8^{+} luminal BCs. Taken together, these data suggest that BCAM^{hi} and BCAM^{lo} BCs defined here represent earlier stages of differentiation than do previously identified KRT8^{+} BCs.

In human sinonasal BC cultures, we found that IL-4/IL-13 upregulates the expression of BCAM and P63 while reducing Notch activity and expression of *SCGB1A1*, which marks differentiated club EpCs. IL-4/IL-13–elicited upregulation of BCAM and P63 was not mediated by STAT6 or mTOR signaling, but was reduced with an inhibitor of IRS-1 and IRS-2, each of which contributes to IL-4R–dependent functions in hematopoietic cells.[87–89] IRS-1 has a demonstrated role in promoting murine embryonic stem cell survival *in vitro*[90] and in maintaining the $Sox9^+$ intestinal stem cell pool *in vivo*,[91] indicating that this is a likely mediator of IL-4/IL-13–elicited stem function. Notably, a role for IL-4/IL-13 in reinforcing stem function was not expected, because previous studies have demonstrated that IL-4/IL-13 drives the differentiation of EpCs to goblet cells.[92,93] Furthermore, T2 cytokine–driven maintenance of the $BCAM^{hi}$ BC stem state has potential significant pathobiological sequelae, because we find that many epithelial mediators of T2 inflammation including *IL33, TSLP, ALOX15*, and *CCL26*[94] are expressed in this cell type. Taken together, these data highlight the potential for T2 cytokines to drive a type of airway remodeling that in turn supports persistent disease.

In this study, we found that the expansion of BCs in the T2 inflammatory disease CRSwNP that we previously reported[13] is due to an increase in the $BCAM^{hi}$ BC subset. Furthermore, we found that *IL4RA, IRS1, TP63*, and TP63-dependent genes were significantly upregulated in CRSwNP, as compared with CRSsNP. Although there is no hallmark gene set to detect enrichment in IRS signaling, we did find that the signature of downstream Akt signaling was highly correlated with a T2-cytokine score across the spectrum of chronic rhinosinusitis (see Fig E6 in this article's Online Repository at www.jacionline.org). Further studies will be needed to define the importance of IRS1 in CRSwNP and whether specific downstream IRS-dependent pathways may be germane therapeutic targets.

Together, our data demonstrate (1) the transcriptional and functional distinctions between multipotent progenitor $BCAM^{hi}$ BCs and their immediate $BCAM^{lo}$ BC descendants, (2) the expansion of $BCAM^{hi}$ BCs in a T2-high disease (CRSwNP), and (3) the IRS signaling pathway through which the T2 cytokines IL-4 and IL-13 can promote stem function. These findings highlight a role for T2 cytokines in the epithelium beyond canonical goblet cell metaplasia and support a growing literature demonstrating a role for T2 cytokines in tissue repair across diverse cell types.[95–97] Moreover, resolving the cell surface phenotype of these early airway EpC precursors provides an opportunity to isolate and assess the molecular features of dysplastic BCs that are increasingly detected in a range of airway diseases from CRSwNP[13] to chronic obstructive pulmonary disease[98] and idiopathic pulmonary fibrosis.[63,99]

Supplementary Material

Refer to Web version on PubMed Central for supplementary material.

Acknowledgments

This work was supported by the National Institutes of Health (grant no. U19AI095219 to J.A.B., N.A.B., T.M.L., S.R., and M.G.A. and grant nos. R01AI134989 and R01HL120952 to N.A.B.), and by the generous support of the Vinik Family Foundation and the Kaye Innovation fund.

We acknowledge Juying Lai for help with sample preparation and Adam Chicoine in the Center for Cellular Profiling for help with sorting.

Abbreviations used

ALI	Air-liquid interface culture
ALT	*Alternaria alternata*
BC	Basal cell
BCAM	Basal cell adhesion molecule
CRSsNP	Chronic rhinosinusitis sans nasal polyposis
CRSwNP	Chronic rhinosinusitis with nasal polyposis
EpC	Epithelial cell
EpCAM	Epithelial cell adhesion molecule
GSIB4	Griffonia simplicifolia lectin B4
IRS	Insulin receptor substrate
ITGA6	Integrin alpha 6
KRT5	Keratin 5
mTOR	Mammalian target of rapamycin
MUC5AC	Mucin 5AC
NGFR	Nerve growth factor receptor
SCGB1A1	Secretoglobin family 1A
scRNA-seq	Single-cell RNA sequencing
SSEA1	Stage-specific mouse embryonic antigen 1
STAT6	Signal transducer and activator of transcription 6
TP63	Tumor protein 63
T2	Type 2

REFERENCES

1. Marillier RG, Michels C, Smith EM, Fick LC, Leeto M, Dewals B, et al. IL-4/IL-13 independent goblet cell hyperplasia in experimental helminth infections. BMC Immunol 2008;9:11. [PubMed: 18373844]
2. Oeser K, Schwartz C, Voehringer D. Conditional IL-4/IL-13-deficient mice reveal a critical role of innate immune cells for protective immunity against gastrointestinal helminths. Mucosal Immunol 2015;8:672–82. [PubMed: 25336167]
3. Birchenough GM, Johansson ME, Gustafsson JK, Bergstrom JH, Hansson GC. New developments in goblet cell mucus secretion and function. Mucosal Immunol 2015;8:712–9. [PubMed: 25872481]
4. Carraro G, Langerman J, Sabri S, Lorenzana Z, Purkayastha A, Zhang G, et al. Transcriptional analysis of cystic fibrosis airways at single-cell resolution reveals altered epithelial cell states and composition. Nat Med 2021;27:806–14. [PubMed: 33958799]
5. Patel NN, Triantafillou V, Maina IW, Workman AD, Tong CCL, Kuan EC, et al. Fungal extracts stimulate solitary chemosensory cell expansion in noninvasive fungal rhinosinusitis. Int Forum Allergy Rhinol 2019;9:730–7. [PubMed: 30892837]
6. Kohanski MA, Workman AD, Patel NN, Hung LY, Shtraks JP, Chen B, et al. Solitary chemosensory cells are a primary epithelial source of IL-25 in patients with chronic rhinosinusitis with nasal polyps. J Allergy Clin Immunol 2018;142:460–9.e7. [PubMed: 29778504]
7. Patel NN, Kohanski MA, Maina IW, Triantafillou V, Workman AD, Tong CCL, et al. Solitary chemosensory cells producing interleukin-25 and group-2 innate lymphoid cells are enriched in chronic rhinosinusitis with nasal polyps [published online ahead of print May 9, 2018]. Int Forum Allergy Rhinol. 10.1002/alr.22142.
8. Aguayo SM, Miller YE, Waldron JA Jr, Bogin RM, Sunday ME, Staton GW Jr, et al. Brief report: idiopathic diffuse hyperplasia of pulmonary neuroendocrine cells and airways disease. N Engl J Med 1992;327:1285–8. [PubMed: 1406819]
9. Davies SJ, Gosney JR, Hansell DM, Wells AU, du Bois RM, Burke MM, et al. Diffuse idiopathic pulmonary neuroendocrine cell hyperplasia: an underrecognised spectrum of disease. Thorax 2007;62:248–52. [PubMed: 17099078]
10. Rossi G, Cavazza A, Spagnolo P, Sverzellati N, Longo L, Jukna A, et al. Diffuse idiopathic pulmonary neuroendocrine cell hyperplasia syndrome. Eur Respir J 2016;47:1829–41. [PubMed: 27076588]
11. Sui P, Wiesner DL, Xu J, Zhang Y, Lee J, Van Dyken S, et al. Pulmonary neuroendocrine cells amplify allergic asthma responses. Science 2018;360:eaan8546. [PubMed: 29599193]
12. Young LR, Brody AS, Inge TH, Acton JD, Bokulic RE, Langston C, et al. Neuroendocrine cell distribution and frequency distinguish neuroendocrine cell hyperplasia of infancy from other pulmonary disorders. Chest 2011;139:1060–71. [PubMed: 20884725]
13. Ordovas-Montanes J, Dwyer DF, Nyquist SK, Buchheit KM, Vukovic M, Deb C, et al. Allergic inflammatory memory in human respiratory epithelial progenitor cells. Nature 2018;560:649–54. [PubMed: 30135581]
14. Vieira Braga FA, Kar G, Berg M, Carpaij OA, Polanski K, Simon LM, et al. A cellular census of human lungs identifies novel cell states in health and in asthma. Nat Med 2019;25:1153–63. [PubMed: 31209336]
15. Travaglini KJ, Nabhan AN, Penland L, Sinha R, Gillich A, Sit RV, et al. A molecular cell atlas of the human lung from single-cell RNA sequencing. Nature 2020;587:619–25. [PubMed: 33208946]
16. Bachert C, Han JK, Desrosiers M, Hellings PW, Amin N, Lee SE, et al. Efficacy and safety of dupilumab in patients with severe chronic rhinosinusitis with nasal polyps (LIBERTY NP SINUS-24 and LIBERTY NP SINUS-52): results from two multicentre, randomised, double-blind, placebo-controlled, parallel-group phase 3 trials. Lancet 2019;394:1638–50. [PubMed: 31543428]
17. Korsunsky I, Millard N, Fan J, Slowikowski K, Zhang F, Wei K, et al. Fast, sensitive and accurate integration of single-cell data with Harmony. Nat Methods 2019;16:1289–96. [PubMed: 31740819]

18. Rock JR, Onaitis MW, Rawlins EL, Lu Y, Clark CP, Xue Y, et al. Basal cells as stem cells of the mouse trachea and human airway epithelium. Proc Natl Acad Sci U S A 2009;106:12771–5. [PubMed: 19625615]
19. Melino G, Memmi EM, Pelicci PG, Bernassola F. Maintaining epithelial stemness with p63. Sci Signal 2015;8:re9. [PubMed: 26221054]
20. Memmi EM, Sanarico AG, Giacobbe A, Peschiaroli A, Frezza V, Cicalese A, et al. p63 sustains self-renewal of mammary cancer stem cells through regulation of Sonic Hedgehog signaling. Proc Natl Acad Sci U S A 2015;112:3499–504. [PubMed: 25739959]
21. Thapa R, Wilson GD. The importance of CD44 as a stem cell biomarker and therapeutic target in cancer. Stem Cells Int 2016;2016:2087204. [PubMed: 27200096]
22. Amodio N, Raimondi L, Juli G, Stamato MA, Caracciolo D, Tagliaferri P, et al. MALAT1: a druggable long non-coding RNA for targeted anti-cancer approaches. J Hematol Oncol 2018;11:63. [PubMed: 29739426]
23. Gomi K, Arbelaez V, Crystal RG, Walters MS. Activation of NOTCH1 or NOTCH3 signaling skews human airway basal cell differentiation toward a secretory pathway. PLoS One 2015;10:e0116507. [PubMed: 25700162]
24. Watson JK, Rulands S, Wilkinson AC, Wuidart A, Ousset M, Van Keymeulen A, et al. Clonal dynamics reveal two distinct populations of basal cells in slow-turnover airway epithelium. Cell Rep 2015;12:90–101. [PubMed: 26119728]
25. Rawlins EL, Okubo T, Xue Y, Brass DM, Auten RL, Hasegawa H, et al. The role of Scgb1a11 Clara cells in the long-term maintenance and repair of lung airway, but not alveolar, epithelium. Cell Stem Cell 2009;4:525–34. [PubMed: 19497281]
26. LeSimple P, van Seuningen I, Buisine MP, Copin MC, Hinz M, Hoffmann W, et al. Trefoil factor family 3 peptide promotes human airway epithelial ciliated cell differentiation. Am J Respir Cell Mol Biol 2007;36:296–303. [PubMed: 17008636]
27. Revinski DR, Zaragosi LE, Boutin C, Ruiz-Garcia S, Deprez M, Thome V, et al. CDC20B is required for deuterosome-mediated centriole production in multiciliated cells. Nat Commun 2018;9:4668. [PubMed: 30405130]
28. Mo JS, Yu FX, Gong R, Brown JH, Guan KL. Regulation of the Hippo-YAP pathway by protease-activated receptors (PARs). Genes Dev 2012;26:2138–43. [PubMed: 22972936]
29. Wang J, Song W, Yang R, Li C, Wu T, Dong XB, et al. Endothelial Wnts control mammary epithelial patterning via fibroblast signaling. Cell Rep 2021;34:108897. [PubMed: 33789106]
30. Yochum GS, Sherrick CM, Macpartlin M, Goodman RH. A beta-catenin/TCF-coordinated chromatin loop at MYC integrates 5' and 3' Wnt responsive enhancers. Proc Natl Acad Sci U S A 2010;107:145–50. [PubMed: 19966299]
31. Rock JR, Gao X, Xue Y, Randell SH, Kong YY, Hogan BL. Notch-dependent differentiation of adult airway basal stem cells. Cell Stem Cell 2011;8:639–48. [PubMed: 21624809]
32. Sanchez-Solana B, Nueda ML, Ruvira MD, Ruiz-Hidalgo MJ, Monsalve EM, Rivero S, et al. The EGF-like proteins DLK1 and DLK2 function as inhibitory non-canonical ligands of NOTCH1 receptor that modulate each other's activities. Biochim Biophys Acta 2011;1813:1153–64. [PubMed: 21419176]
33. Zhang L, Prak L, Rayon-Estrada V, Thiru P, Flygare J, Lim B, et al. ZFP36L2 is required for self-renewal of early burst-forming unit erythroid progenitors. Nature 2013;499:92–6. [PubMed: 23748442]
34. Yi S, Yu M, Yang S, Miron RJ, Zhang Y. Tcf12, a member of basic helix-loop-helix transcription factors, mediates bone marrow mesenchymal stem cell osteogenic differentiation in vitro and in vivo. Stem Cells 2017;35:386–97. [PubMed: 27574032]
35. Warner SM, Hackett TL, Shaheen F, Hallstrand TS, Kicic A, Stick SM, et al. Transcription factor p63 regulates key genes and wound repair in human airway epithelial basal cells. Am J Respir Cell Mol Biol 2013;49:978–88. [PubMed: 23837456]
36. Byers DE, Alexander-Brett J, Patel AC, Agapov E, Dang-Vu G, Jin X, et al. Longterm IL-33-producing epithelial progenitor cells in chronic obstructive lung disease. J Clin Invest 2013;123:3967–82. [PubMed: 23945235]

37. Carriere V, Roussel L, Ortega N, Lacorre DA, Americh L, Aguilar L, et al. IL-33, the IL-1-like cytokine ligand for ST2 receptor, is a chromatin-associated nuclear factor in vivo. Proc Natl Acad Sci U S A 2007;104:282–7. [PubMed: 17185418]
38. Woodruff PG, Modrek B, Choy DF, Jia G, Abbas AR, Ellwanger A, et al. T-helper type 2-driven inflammation defines major subphenotypes of asthma. Am J Respir Crit Care Med 2009;180:388–95. [PubMed: 19483109]
39. Brembeck FH, Opitz OG, Libermann TA, Rustgi AK. Dual function of the epithelial specific ets transcription factor, ELF3, in modulating differentiation. Oncogene 2000;19:1941–9. [PubMed: 10773884]
40. Ng AY, Waring P, Ristevski S, Wang C, Wilson T, Pritchard M, et al. Inactivation of the transcription factor Elf3 in mice results in dysmorphogenesis and altered differentiation of intestinal epithelium. Gastroenterology 2002;122:1455–66. [PubMed: 11984530]
41. Margadant C, Frijns E, Wilhelmsen K, Sonnenberg A. Regulation of hemidesmosome disassembly by growth factor receptors. Curr Opin Cell Biol 2008;20:589–96. [PubMed: 18583123]
42. Alysandratos KD, Herriges MJ, Kotton DN. Epithelial stem and progenitor cells in lung repair and regeneration. Annu Rev Physiol 2021;83:529–50. [PubMed: 33074772]
43. Davis JD, Wypych TP. Cellular and functional heterogeneity of the airway epithelium. Mucosal Immunol 2021;14:978–90. [PubMed: 33608655]
44. Shimizu T, Nettesheim P, Mahler JF, Randell SH. Cell type-specific lectin staining of the tracheobronchial epithelium of the rat: quantitative studies with *Griffonia simplicifolia* I isolectin B4. J Histochem Cytochem 1991;39:7–14. [PubMed: 1701188]
45. Zhao R, Fallon TR, Saladi SV, Pardo-Saganta A, Villoria J, Mou H, et al. Yap tunes airway epithelial size and architecture by regulating the identity, maintenance, and self-renewal of stem cells. Dev Cell 2014;30:151–65. [PubMed: 25043474]
46. Mark M, Rijli FM, Chambon P. Homeobox genes in embryogenesis and pathogenesis. Pediatr Res 1997;42:421–9. [PubMed: 9380431]
47. Oda Y, Hu L, Nguyen T, Fong C, Zhang J, Guo P, et al. Vitamin D receptor is required for proliferation, migration, and differentiation of epidermal stem cells and progeny during cutaneous wound repair. J Invest Dermatol 2018;138:2423–31. [PubMed: 29787748]
48. Brockman-Schneider RA, Pickles RJ, Gern JE. Effects of vitamin D on airway epithelial cell morphology and rhinovirus replication. PLoS One 2014;9:e86755. [PubMed: 24475177]
49. Memon A, Lee WK. KLF10 as a tumor suppressor gene and its TGF-beta signaling. Cancers (Basel) 2018;10:161. [PubMed: 29799499]
50. Wang Y, Wu J, Chen H, Yang Y, Xiao C, Yi X, et al. Genome-wide CRISPR-Cas9 screen identified KLF11 as a druggable suppressor for sarcoma cancer stem cells. Sci Adv 2021;7:eabe3445. [PubMed: 33571129]
51. Aubrey BJ, Strasser A, Kelly GL. Tumor-suppressor functions of the TP53 pathway. Cold Spring Harb Perspect Med 2016;6:a026062. [PubMed: 27141080]
52. Riege K, Kretzmer H, Sahm A, McDade SS, Hoffmann S, Fischer M. Dissecting the DNA binding landscape and gene regulatory network of p63 and p53. Elife 2020;9:e63266. [PubMed: 33263276]
53. Kubo T, Sato S, Hida T, Minowa T, Hirohashi Y, Tsukahara T, et al. IL-13 modulates Np63 levels causing altered expression of barrier- and inflammation-related molecules in human keratinocytes: a possible explanation for chronicity of atopic dermatitis. Immun Inflamm Dis 2021;9:734–45. [PubMed: 33792188]
54. Mou H, Vinarsky V, Tata PR, Brazauskas K, Choi SH, Crooke AK, et al. Dual SMAD signaling inhibition enables long-term expansion of diverse epithelial basal cells. Cell Stem Cell 2016;19:217–31. [PubMed: 27320041]
55. White SR, Martin LD, Abe MK, Marroquin BA, Stern R, Fu X. Insulin receptor substrate-1/2 mediates IL-4-induced migration of human airway epithelial cells. Am J Physiol Lung Cell Mol Physiol 2009;297:L164–73. [PubMed: 19447894]
56. Bonser LR, Koh KD, Johansson K, Choksi SP, Cheng D, Liu L, et al. Flow-cytometric analysis and purification of airway epithelial-cell subsets. Am J Respir Cell Mol Biol 2021;64:308–17. [PubMed: 33196316]

57. Pardo-Saganta A, Law BM, Tata PR, Villoria J, Saez B, Mou H, et al. Injury induces direct lineage segregation of functionally distinct airway basal stem/progenitor cell subpopulations. Cell Stem Cell 2015;16:184–97. [PubMed: 25658372]
58. Pardo-Saganta A, Tata PR, Law BM, Saez B, Chow RD, Prabhu M, et al. Parent stem cells can serve as niches for their daughter cells. Nature 2015;523:597–601. [PubMed: 26147083]
59. Montoro DT, Haber AL, Biton M, Vinarsky V, Lin B, Birket SE, et al. A revised airway epithelial hierarchy includes CFTR-expressing ionocytes. Nature 2018;560:319–24. [PubMed: 30069044]
60. Ghosh M, Ahmad S, Jian A, Li B, Smith RW, Helm KM, et al. Human tracheobronchial basal cells. Normal versus remodeling/repairing phenotypes in vivo and in vitro. Am J Respir Cell Mol Biol 2013;49:1127–34. [PubMed: 23927678]
61. Plasschaert LW, Zilionis R, Choo-Wing R, Savova V, Knehr J, Roma G, et al. A single-cell atlas of the airway epithelium reveals the CFTR-rich pulmonary ionocyte. Nature 2018;560:377–81. [PubMed: 30069046]
62. Mou H, Yang Y, Riehs MA, Barrios J, Shivaraju M, Haber AL, et al. Airway basal stem cells generate distinct subpopulations of PNECs. Cell Rep 2021;35:109011. [PubMed: 33882306]
63. Carraro G, Mulay A, Yao C, Mizuno T, Konda B, Petrov M, et al. Single-cell reconstruction of human basal cell diversity in normal and idiopathic pulmonary fibrosis lungs. Am J Respir Crit Care Med 2020;202:1540–50. [PubMed: 32692579]
64. Hibi K, Fujitake S, Takase T, Kodera Y, Ito K, Akiyama S, et al. Identification of S100A2 as a target of the DeltaNp63 oncogenic pathway. Clin Cancer Res 2003;9:4282–5. [PubMed: 14519656]
65. Kirschner RD, Sanger K, Muller GA, Engeland K. Transcriptional activation of the tumor suppressor and differentiation gene S100A2 by a novel p63-binding site. Nucleic Acids Res 2008;36:2969–80. [PubMed: 18388131]
66. Lapi E, Iovino A, Fontemaggi G, Soliera AR, Iacovelli S, Sacchi A, et al. S100A2 gene is a direct transcriptional target of p53 homologues during keratinocyte differentiation. Oncogene 2006;25:3628–37. [PubMed: 16449968]
67. Justilien V, Regala RP, Tseng IC, Walsh MP, Batra J, Radisky ES, et al. Matrix metalloproteinase-10 is required for lung cancer stem cell maintenance, tumor initiation and metastatic potential. PLoS One 2012;7:e35040. [PubMed: 22545096]
68. Mariya T, Hirohashi Y, Torigoe T, Tabuchi Y, Asano T, Saijo H, et al. Matrix metalloproteinase-10 regulates stemness of ovarian cancer stem-like cells by activation of canonical Wnt signaling and can be a target of chemotherapy-resistant ovarian cancer. Oncotarget 2016;7:26806–22. [PubMed: 27072580]
69. Zhang H, Pan YZ, Cheung M, Cao M, Yu C, Chen L, et al. LAMB3 mediates apoptotic, proliferative, invasive, and metastatic behaviors in pancreatic cancer by regulating the PI3K/Akt signaling pathway. Cell Death Dis 2019;10:230. [PubMed: 30850586]
70. Moumen M, Chiche A, Decraene C, Petit V, Gandarillas A, Deugnier MA, et al. Myc is required for beta-catenin-mediated mammary stem cell amplification and tumorigenesis. Mol Cancer 2013;12:132. [PubMed: 24171719]
71. Quan T, Xu Y, Qin Z, Robichaud P, Betcher S, Calderone K, et al. Elevated YAP and its downstream targets CCN1 and CCN2 in basal cell carcinoma: impact on keratinocyte proliferation and stromal cell activation. Am J Pathol 2014;184:937–43. [PubMed: 24485923]
72. Deprez M, Zaragosi LE, Truchi M, Becavin C, Ruiz Garcia S, Arguel MJ, et al. A single-cell atlas of the human healthy airways. Am J Respir Crit Care Med 2020;202:1636–45. [PubMed: 32726565]
73. Parsons SF, Lee G, Spring FA, Willig TN, Peters LL, Gimm JA, et al. Lutheran blood group glycoprotein and its newly characterized mouse homologue specifically bind alpha5 chain-containing human laminin with high affinity. Blood 2001;97:312–20. [PubMed: 11133776]
74. Udani M, Zen Q, Cottman M, Leonard N, Jefferson S, Daymont C, et al. Basal cell adhesion molecule/lutheran protein. The receptor critical for sickle cell adhesion to laminin. J Clin Invest 1998;101:2550–8. [PubMed: 9616226]

75. Kikkawa Y, Ogawa T, Sudo R, Yamada Y, Katagiri F, Hozumi K, et al. The lutheran/basal cell adhesion molecule promotes tumor cell migration by modulating integrin-mediated cell attachment to laminin-511 protein. J Biol Chem 2013;288:30990–1001. [PubMed: 24036115]
76. Chang HY, Chang HM, Wu TJ, Chaing CY, Tzai TS, Cheng HL, et al. The role of Lutheran/basal cell adhesion molecule in human bladder carcinogenesis. J Biomed Sci 2017;24:61. [PubMed: 28841878]
77. Miura Y, Matsui S, Miyata N, Harada K, Kikkawa Y, Ohmuraya M, et al. Differential expression of Lutheran/BCAM regulates biliary tissue remodeling in ductular reaction during liver regeneration. Elife 2018;7:e36572. [PubMed: 30059007]
78. Eenjes E, Mertens TCJ, Buscop-van Kempen MJ, van Wijck Y, Taube C, Rottier RJ, et al. A novel method for expansion and differentiation of mouse tracheal epithelial cells in culture. Sci Rep 2018;8:7349. [PubMed: 29743551]
79. Horani A, Nath A, Wasserman MG, Huang T, Brody SL. Rho-associated protein kinase inhibition enhances airway epithelial basal-cell proliferation and lentivirus transduction. Am J Respir Cell Mol Biol 2013;49:341–7. [PubMed: 23713995]
80. Kikkawa Y, Sudo R, Kon J, Mizuguchi T, Nomizu M, Hirata K, et al. Laminin alpha 5 mediates ectopic adhesion of hepatocellular carcinoma through integrins and/or Lutheran/basal cell adhesion molecule. Exp Cell Res 2008;314:2579–90. [PubMed: 18635166]
81. Laperle A, Hsiao C, Lampe M, Mortier J, Saha K, Palecek SP, et al. Alpha-5 laminin synthesized by human pluripotent stem cells promotes self-renewal. Stem Cell Reports 2015;5:195–206. [PubMed: 26235893]
82. Godavarthy PS, Walter CB, Lengerke C, Klein G. The laminin receptors basal cell adhesion molecule/lutheran and integrin alpha7beta1 on human hematopoietic stem cells. Front Cell Dev Biol 2021;9:675240. [PubMed: 34746117]
83. Ritie L, Spenle C, Lacroute J, Bolcato-Bellemin AL, Lefebvre O, Bole-Feysot C, et al. Abnormal Wnt and PI3Kinase signaling in the malformed intestine of lama5 deficient mice. PLoS One 2012;7:e37710. [PubMed: 22666383]
84. Lepage M, Seltana A, Thibault MP, Tremblay E, Beaulieu JF. Knockdown of laminin alpha5 stimulates intestinal cell differentiation. Biochem Biophys Res Commun 2018;495:1510–5. [PubMed: 29198708]
85. Kouwenhoven EN, van Heeringen SJ, Tena JJ, Oti M, Dutilh BE, Alonso ME, et al. Genome-wide profiling of p63 DNA-binding sites identifies an element that regulates gene expression during limb development in the 7q21 SHFM1 locus. PLoS Genet 2010;6:e1001065. [PubMed: 20808887]
86. Sasamoto Y, Lee CAA, Wilson BJ, Buerger F, Martin G, Mishra A, et al. Limbal BCAM expression identifies a proliferative progenitor population capable of holoclone formation and corneal differentiation. Cell Rep 2022;40:111166. [PubMed: 35947947]
87. Heller NM, Qi X, Junttila IS, Shirey KA, Vogel SN, Paul WE, et al. Type I IL-4Rs selectively activate IRS-2 to induce target gene expression in macrophages. Sci Signal 2008;1:ra17. [PubMed: 19109239]
88. Wang LM, Myers MG Jr, Sun XJ, Aaronson SA, White M, Pierce JH. IRS-1: essential for insulin- and IL-4-stimulated mitogenesis in hematopoietic cells. Science 1993;261:1591–4. [PubMed: 8372354]
89. Sun XJ, Wang LM, Zhang Y, Yenush L, Myers MG Jr, Glasheen E, et al. Role of IRS-2 in insulin and cytokine signalling. Nature 1995;377:173–7. [PubMed: 7675087]
90. Rubin R, Arzumanyan A, Soliera AR, Ross B, Peruzzi F, Prisco M. Insulin receptor substrate (IRS)-1 regulates murine embryonic stem (mES) cells self-renewal. J Cell Physiol 2007;213:445–53. [PubMed: 17620314]
91. Ramocki NM, Wilkins HR, Magness ST, Simmons JG, Scull BP, Lee GH, et al. Insulin receptor substrate-1 deficiency promotes apoptosis in the putative intestinal crypt stem cell region, limits Apcmin/1 tumors, and regulates Sox9. Endocrinology 2008;149:261–7. [PubMed: 17916629]
92. Wills-Karp M, Luyimbazi J, Xu X, Schofield B, Neben TY, Karp CL, et al. Interleukin-13: central mediator of allergic asthma. Science 1998;282:2258–61. [PubMed: 9856949]

93. Grunig G, Warnock M, Wakil AE, Venkayya R, Brombacher F, Rennick DM, et al. Requirement for IL-13 independently of IL-4 in experimental asthma. Science 1998;282:2261–3. [PubMed: 9856950]

94. Hewitt RJ, Lloyd CM. Regulation of immune responses by the airway epithelial cell landscape. Nat Rev Immunol 2021;21:347–62. [PubMed: 33442032]

95. Goh YP, Henderson NC, Heredia JE, Red Eagle A, Odegaard JI, Lehwald N, et al. Eosinophils secrete IL-4 to facilitate liver regeneration. Proc Natl Acad Sci U S A 2013;110:9914–9. [PubMed: 23716700]

96. Heredia JE, Mukundan L, Chen FM, Mueller AA, Deo RC, Locksley RM, et al. Type 2 innate signals stimulate fibro/adipogenic progenitors to facilitate muscle regeneration. Cell 2013;153:376–88. [PubMed: 23582327]

97. Walsh JT, Hendrix S,Boato F, Smirnov I, Zheng J, Lukens JR, et al. MHCII-independent CD4+ T cells protect injured CNS neurons via IL-4. J Clin Invest 2015;125:2547.

98. Ghosh M, Miller YE, Nakachi I, Kwon JB, Baron AE, Brantley AE, et al. Exhaustion of airway basal progenitor cells in early and established chronic obstructive pulmonary disease. Am J Respir Crit Care Med 2018;197:885–96. [PubMed: 29211494]

99. Adams TS, Schupp JC, Poli S, Ayaub EA, Neumark N, Ahangari F, et al. Single-cell RNA-seq reveals ectopic and aberrant lung-resident cell populations in idiopathic pulmonary fibrosis. Sci Adv 2020;6:eaba1983. [PubMed: 32832599]

Key messages

- Two subsets of airway BCs have distinct transcriptional signatures and function.
- High levels of BCAM expression mark the earliest BC progenitor.
- IL-4 and IL-13 upregulate BCAM and P63 in an IRS-dependent fashion that prevents BC differentiation to secretory EpCs.
- $BCAM^{hi}$ BCs are increased in CRSwNP.

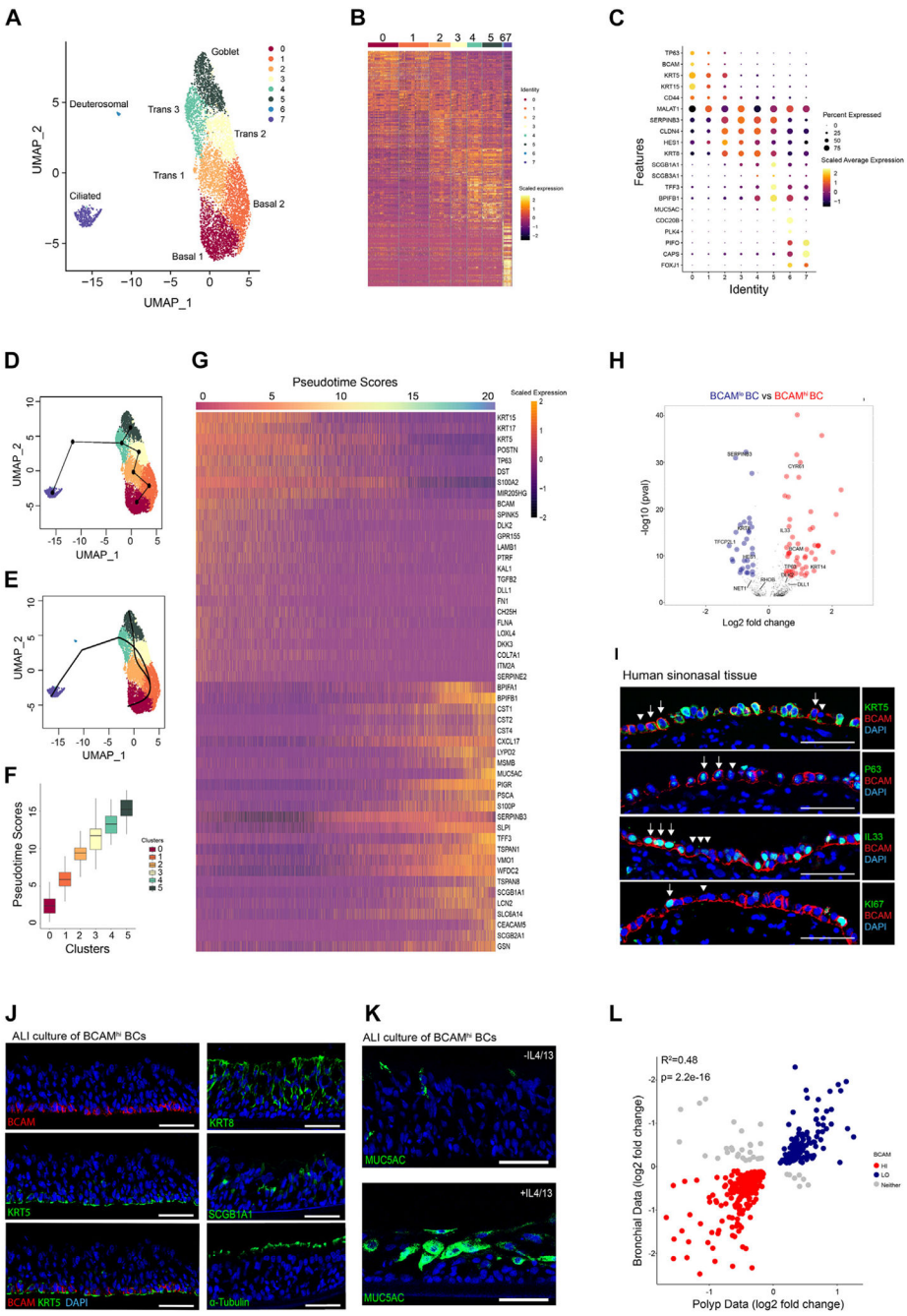

FIG 1.

BCAM marks a multipotent progenitor among KRT5^{+}NGFR^{+}ITGA6^{+} BCs in the human respiratory mucosa. **A,** UMAP representation of 6970 EpCs from 12 donors. **B,** Heatmap of scaled gene expression for the top 30 genes identified by Wilcoxon rank-sum test and auROC analysis. **C,** Dot plot of epithelial markers across clusters. **D,** Cluster-based minimum spanning tree of lineages overlaid on UMAP. **E,** Cell assignment to smooth principal curves with lineage-specific pseudotimes. **F,** Plot of pseudotime scores from cells assigned to the secretory lineage. **G,** Heatmap of scaled gene expression for the topmost

significant genes associated with changes in pseudotime (Bonferroni-corrected *P* values). **H,** Volcano plot of log2 fold change between basal 0 ($BCAM^{hi}$) BCs and basal 1 ($BCAM^{lo}$) BCs. Significant genes with increased expression in $BCAM^{hi}$ (*red*) and $BCAM^{lo}$ (*blue*) ($P < 1.5 \times 10^{-5}$, Bonferroni threshold). **I,** Representative immunostaining of human sinonasal tissue from a patient with CRSwNP. Arrow indicates $BCAM^{hi}$ BCs, and arrowhead indicates $BCAM^{lo}$ BCs. The scale bar represents 50 μm (n = 3). **J,** Representative immunostaining on ALI cultures derived from $BCAM^{hi}$ BCs. The scale bar represents 50 μm (n = 3). **K,** Representative immunostaining on ALI cultures derived from $BCAM^{hi}$ BCs treated with/without IL-4/IL-13 (n = 3). **L,** Coefficient of determination of $\log_2$ fold changes of shared genes from sinonasal BCs ($BCAM^{hi}$ vs $BCAM^{lo}$) and bronchial BCs (BC1 vs BC2). *auROC*, Area under the receiving operator characteristic; *DAPI*, 4'-6-diamidino-2-phenylindole; *UMAP*, uniform manifold approximation and projection.

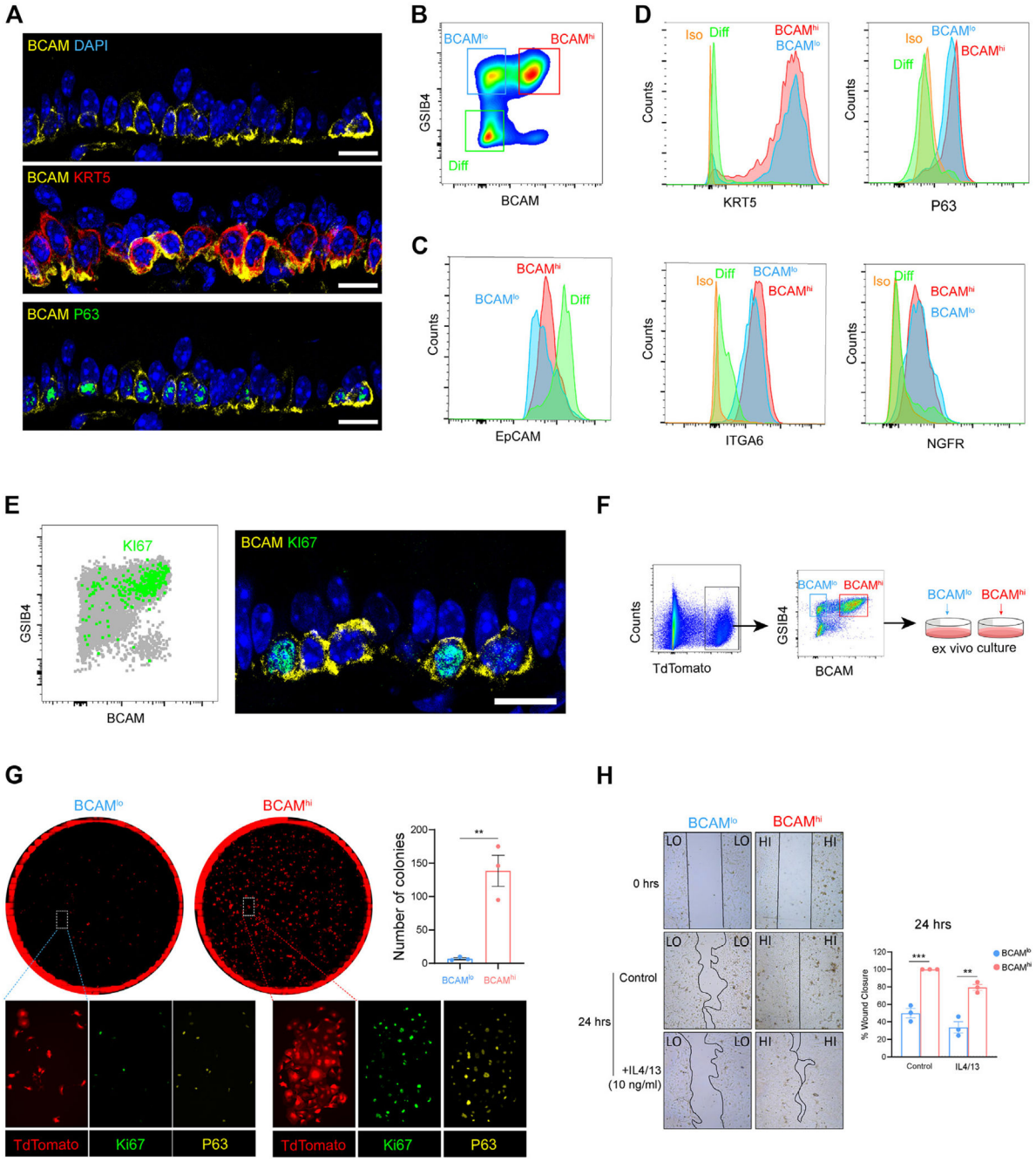

FIG 2.

BCAM marks an airway basal stem cell among KRT5^{+}NGFR^{+}ITGA6^{+}P63^{+} BCs in the naive murine trachea. **A,** Representative immunostaining in naive murine trachea. The scale bar represents 10 μm. **B,** Flow-cytometric panel of BCAM^{hi} BCs, BCAM^{lo} BCs, and differentiated EpCs (Diff). **C,** Expression of EpCAM in each group. **D,** Expression of canonical BC markers in each group. **E,** KI67 expression in naive tracheal airway epithelium assessed by flow-cytometric staining (*left*) and confocal microscopy (*right*). The scale bar represents 10 μm. **F,** Schema depicting the isolation and *ex vivo* culture of BCAM^{hi}

BCs and BCAM^{lo} BCs from KRT5^{CrerERT2}:R26^{tdTomato} mice (for detailed information, see this article's Methods section in the Online Repository at www.jacionline.org). **G,** Colony-forming assay on sorted BCAM^{hi} BCs and BCAM^{lo} BCs with immunostaining. Number of colonies was calculated using image J. Data are shown as mean ± SEM (n = 3; $^{**}P < .01$; unpaired 2-tailed t test). **H,** Wound-healing assay on sorted BCAM^{hi} BCs and BCAM^{lo} BCs in the presence or absence of 10 ng/mL IL-4 and IL-13. Images were taken at 0 and 24 hours. The percentage of wound closure was calculated using image J. Data are shown as mean ± SEM (n = 3; $P < .02$; linear regression). All immunostaining is representative of n = 3. *DAPI,* 4'-6-Diamidino-2-phenylindole.

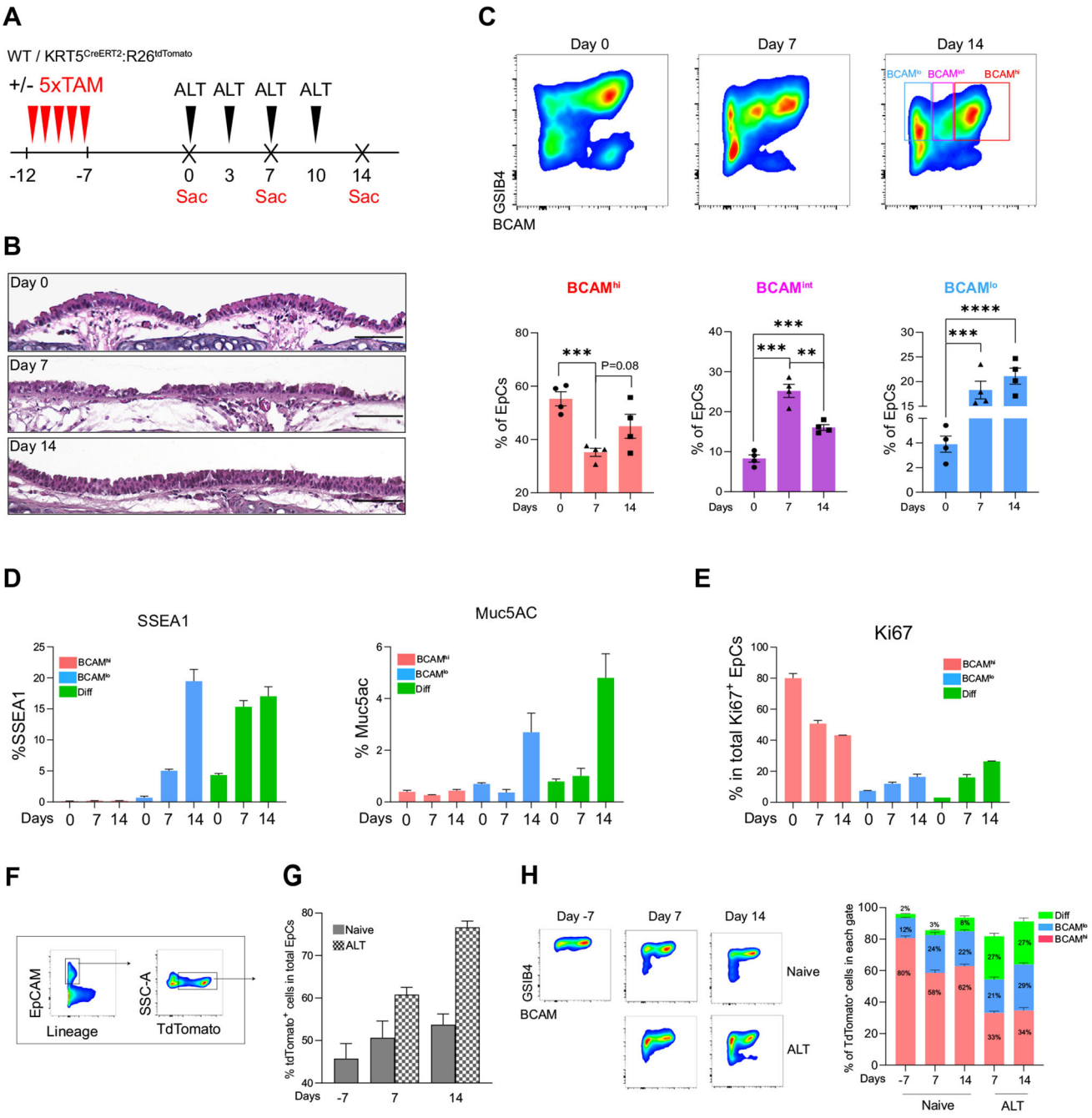

FIG 3.

Fate labeling demonstrates a trajectory from BCAM^{hi} BCs to BCAM^{lo} BCs and then to differentiated EpCs. **A,** Experimental schema. **B,** H&E staining of mouse trachea. The scale bar represents 100 μm. Staining is representative of n = 3. **C,** Flow-cytometric panel showing the percentage of BCAM^{hi} BCs, BCAM^{int} BCs, and BCAM^{lo} BCs in naive and challenged airways. Data are shown as mean ± SEM (n = 4; $^{**}P < .01$, $^{***}P < .001$; unpaired 2-tailed *t* test). **D,** Percentage of SSEA1^{+} cells and MUC5AC^{+} cells in each EpC subset. Data are shown as mean ± SEM (n = 3). **E,** Percentage of Ki67^{+} cells in

each EpC subset. Data are shown as mean ± SEM (n = 3). **F,** Gating strategy identifying tdTomato^{+} EpCs in KRT5^{CrerERT2}:R26^{tdTomato} mice. **G,** Percentage of tdTomato^{+} EpCs out of total EpCs at the indicated time points. Data are shown as mean ± SEM (n = 3). **H,** A representative image of GSIB4 and BCAM staining on tdTomato^{+} EpCs (*left*). Percentage of tdTomato^{+} EpCs that fall within each gate in naive and ALT at the indicated time points (*right*). Data are shown as mean ± SEM (n = 3).

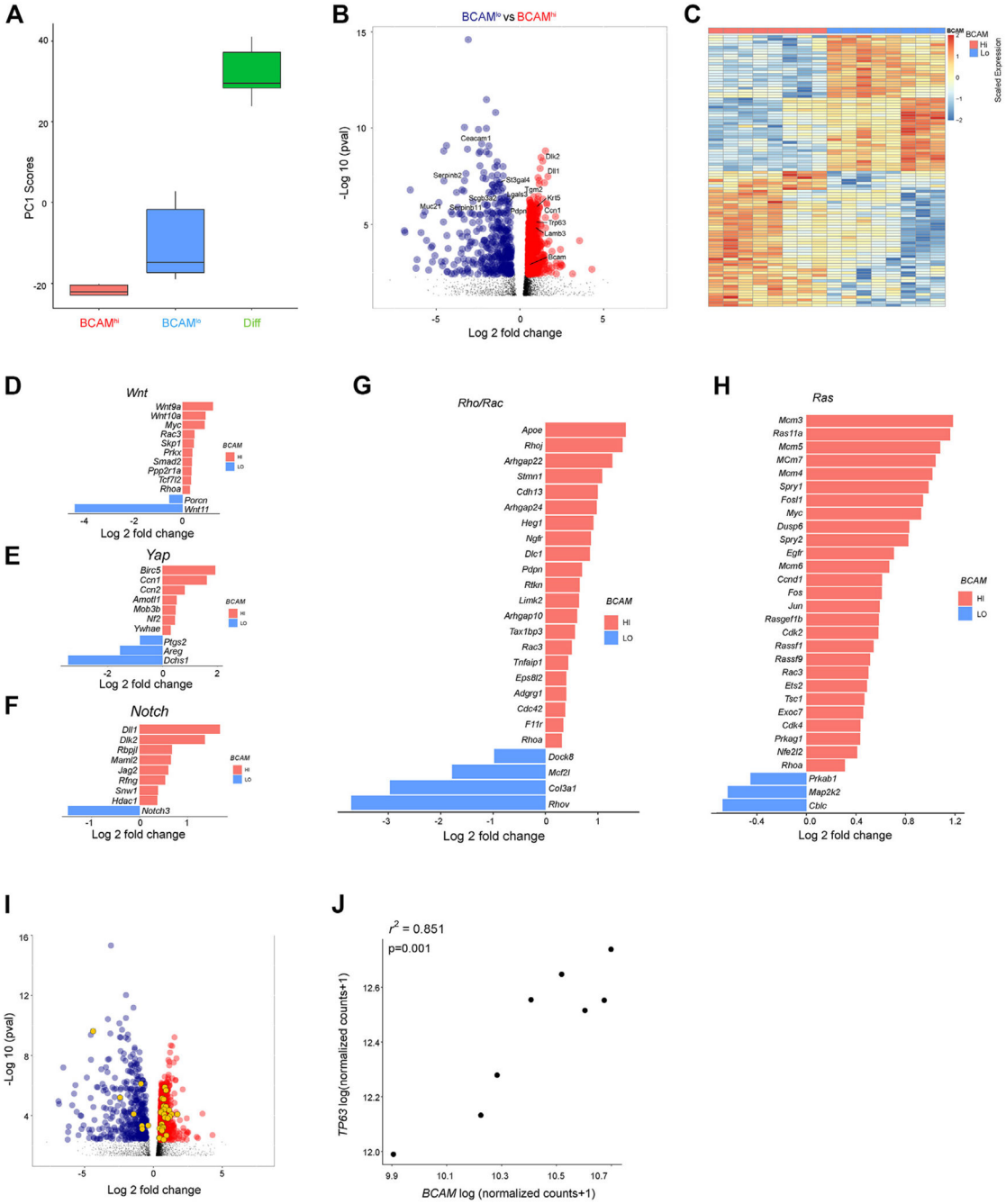

FIG 4.

BCAM^{hi} BCs are enriched in canonical stem cell signaling pathways. **A,** Box plot of principal-component 1 scores from sorted murine BCAM^{hi} BCs, BCAM^{lo} BCs, and differentiated EpCs (Diff). **B,** Volcano plot showing differentially expressed genes in BCAM^{hi} BCs compared with BCAM^{lo} BCs. Highlighted genes are significantly enriched in BCAM^{hi} BCs (*red*) and BCAM^{lo} BCs (*dark blue*), (Benjamini-Hochberg, $P < .05$). **C,** Heatmap of the top 100 most significant differentially expressed genes in BCAM^{hi} BCs and BCAM^{lo} BCs (Benjamini-Hochberg, $P < .05$; see Tables E10 and E11). **D-H,**

Significant differentially expressed genes (Benjamini-Hochberg, $P < .05$) between BCAM^{hi} and BCAM^{lo} BCs associated with *Wnt* signaling (Fig 4, D), *Hippo* signaling (Fig 4, E), *Notch* signaling (Fig 4, F), *Rho/Rock* signaling (Fig 4, G), and *Ras* signaling (Fig 4, H). **I,** Volcano plot showing differentially expressed genes up in BCAM^{hi} BCs (*red*) compared with BCAM^{lo} BCs (*blue*). The significant differentially expressed genes that are P63 target genes are colored in orange. **J,** Correlation between *BCAM* and *TP63* expression (normalized counts; DESeq2 median of ratios) in bulk RNA-seq from human polyp BCs.

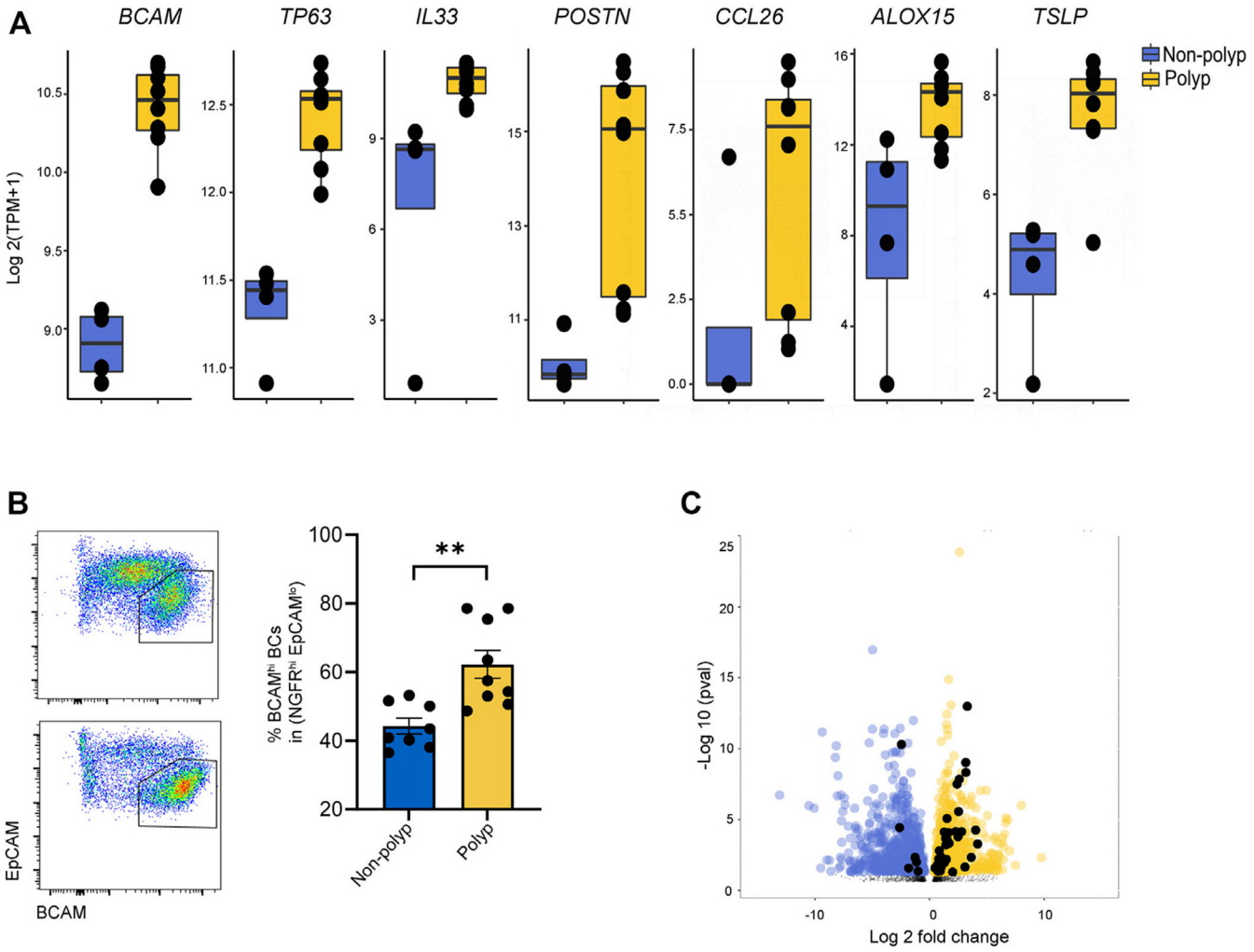

FIG 5.

Expression of BCAM and the P63-dependent stem program is increased in CRSwNP and CRSsNP. **A,** Expression of the indicated genes in bulk RNA-seq from human sinonasal polyp BCs and nonpolyp BC controls. Adjusted *P* value (Benjamini-Hochberg) as follows: *BCAM* = 3.7×10^{-13}, *TP63* = 4.69×10^{-7}, *IL33* = 3.02×10^{-2}, *POSTN* = 5.20×10^{-6}, *CCL26* = 3.44×10^{-1}(not significant), *ALOX15* = 2.95×10^{-2}, and *TSLP* = 9.14×10^{-7}. **B,** Flow cytometry on $lin^{-}EpCAM^{+}$ EpCs from CRSsNP and CRSwNP. Data are shown as mean ± SEM (**$P < .002$; unpaired 2-tailed *t* test). **C,** Volcano plot showing differentially expressed genes up in CRSwNP (*yellow*) compared with CRSsNP (*blue*). The significant differentially expressed genes that are P63 target genes are colored in black. *TPM*, Transcripts per million.

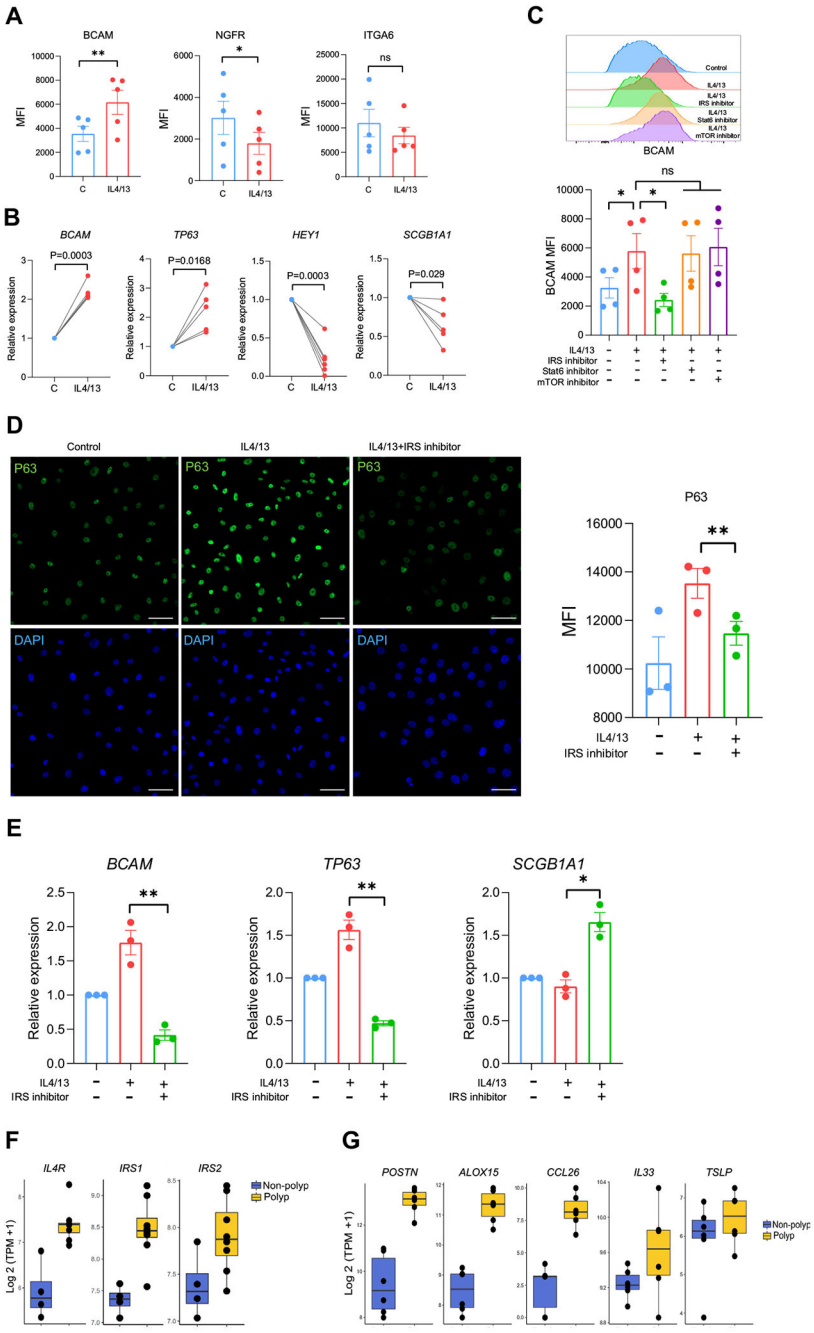

FIG 6.

T2 cytokine–dependent and IRS-dependent regulation of BCAM. **A,** MFI of BCAM, NGFR, and ITGA6. Data are shown as mean ± SEM (**P* < .05, ***P* < .01; paired 2-tailed *t* test). **B,** Quantitative PCR for the indicated genes. Data are shown as mean ± SEM (**P* < .05, **P < .01; paired 2-tailed *t* test). **C,** Histogram (*left*) and MFI quantification (*right*) of BCAM expression in IL-4/IL-13-treated BCs ± inhibitors of IRS-1/2, mTOR, and STAT6. Data are shown as mean ± SEM (**P* < .05; paired 2-tailed *t* test. **D,** Representative images (*left*) and MFI quantification (*right*) of P63 staining on IL-4/IL-13-treated BCs ± an IRS-1/2 inhibitor.

Scale bar = 50 μm. Data are shown as mean ± SEM (*$P < .05$; paired 2-tailed *t* test). **E,** Quantitative PCR on IL-4/IL-13–treated BCs ± an IRS-1/2 inhibitor. Data are shown as mean ± SEM (*$P < .05$, **$P < .01$; paired 2-tailed *t* test). Human sinonasal BCs treated ± 10 ng/mL IL-4/IL-13 (Fig 6, A-E). **F**, Expression of components of IL-4R signaling pathway in bulk BC sequencing from CRSwNP or CRSsNP. *IL4R* and *IRS1* were significantly different (Benjamini-Hochberg–adjusted *P* values < .05). **G,** Expression of the indicated genes in scRNA-seq cluster 0 ($BCAM^{hi}$ BCs) from CRSwNP and CRSsNP. Bonferroni threshold (1.59×10^{-5}) for *POSTN* = 3.21×10^{-7}, *CCL26* = 8.97×10^{-6}, and *ALOX15* = 1.28×10^{-10}. *DAPI*, 4'-6-Diamidino-2-phenylindole; *MFI*, mean fluorescence intensity; *NS*, not significant; *TPM*, transcripts per million.

TABLE I.

Established markers of airway epithelial cells

Cell type	Marker	
BCs	NGFR	Nerve growth factor receptor
	GSIB4 *	Lectin Griffonia simplicifolia IB4
	ITGA6	Integrin subunit alpha 6
	KRT5	Keratin 5
	TP63	Tumor protein 63
	CD44	CD44 molecule
	PDPN	Podoplanin
Luminal progenitor BCs	KRT8	Keratin 8
Secretory club cells	SCGB1A1	Secretoglobin family 1A member 1
Goblet cells	MUC5AC	Mucin 5AC
Ciliated cells	FOXJ1	Forkhead box J1
	Acetyl-α-tubulin	Acetylated alpha tubulin

* GSIB4 lectin is a validated marker of murine, but not human, BCs.